ISSN 2176-5480

22nd International Congress of Mechanical Engineering (COBEM 2013)
November 3-7, 2013, Ribeirão Preto, SP, Brazil

INFLUENCE OF ETHANOL TEMPERATURE ON ATOMIZATION PARAMETERS FROM A MULTI-HOLE PORT FUEL INJECTOR

Renata Fajgenbaum
Rogério Gonçalves dos Santos
University of Campinas, Department of Mechanical Enginnering
200 Mendeleyev st, Barão Geraldo, Campinas, SP, Brazil
fajgenba@fem.unicamp.br
roger7@fem.unicamp.br

Abstract. *The motivation in studying the phenomena that happen in each internal combustion engine subsystem lies in the possibility to predict and optimize its operation. The atomization process that occurs in fuel injectors has a strong relation with the subsequent combustion reaction and thus with the engine thermal efficiency. Experiments were performed to investigate the liquid temperature effect on atomization parameters in an internal combustion engine pressure-swirl atomizer. The experimental apparatus consisted of a flow control rig connected with a heat control system. The flow rig, which is an injection system, was built specifically for that purpose and the heat system goal was to vary the ethanol temperature. The atomization parameters were evaluated by laser diagnostics and the measurements were made by means of Shadowgraphy in order to measure drop mean diameter, velocity field and macroscopic aspects of the spray. The results for drop sizing were expressed in terms of Sauter Mean Diameter (SMD) and the measurements were taken in two different axial distances from the nozzle exit, 25 mm and 100 mm. Previous results showed that SMD as well as velocity field remained insensitive to the range of 10 to 60 ^{o}C fuel temperature as this variation does not provide significant changes in liquid properties.*

Keywords: *atomization, shadowgraphy, SMD, velocity field, ethanol.*

1. INTRODUCTION

Internal combustion engines still represent the main way to obtain energy in automotive field. The studies related to improvement and optimization of engine injection system are directly connected to the reduction of pollutants emission subject. The atomization process has a strong relation with the subsequent combustion reaction and thus with the engine thermal efficiency. Therefore, the specialized study, through experimentation and modeling, allows fuels such as ethanol to be used to combustion in a more efficient way.

Direct injection systems were extensively studied to predict the atomization behavior using different operation conditions. Tests involving variation in injection pressure were conducted by Lee, *et al.*, 2001 and Wang, *et al.*, 2005 where both concluded that an increase in injection pressure causes the SMD to decrease, thus generating a better atomization.

Using fuel viscosity as an input parameter, Chen, *et al.*, 1991 and Goldsworthy, *et al.*, 2011 realized that the higher the value of viscosity the greater the SMD. Aleiferis, *et al.*, 2010 performed experiments varying the fuel temperature and found out that the SMD decreases with increasing temperature. Qualitative atomization analysis, comparing gasoline with ethanol, were made by Gao, *et al.*, 2007 and Park, *et al.*, 2009.

Port fuel injection (PFI) has injection pressure ranges much lower than direct injection so than the spray characteristics is different for each of them. As Anad, *et al.*, 2012 suggest there are no references of ethanol or ethanol blends studies in port fuel injectors and that is why they decided to introduce the subject. Following the same argument, the present study claims for a better understanding of the atomization process involving PFI.

2. EXPERIMENTAL SETUP

2.1 Experimental apparatus

The experimental apparatus consists of a fuel injection system connected with a heat control system and Shadowgraphy equipment.

The apparatus was built aiming to be adapted to the laser diagnostics equipment, therefore a transparent chamber surrounding the fuel injector was made in order to allow visibility of the spray. Fuel is supplied to the nozzle from a tank inside which a serpentine is located and connected to a heat exchanger in order to warm up or chill the fuel. A thermocouple attached to the fuel rail wall gives the temperature used in each test and here called „fuel temperature", thus a settling time of 20 min is used to allow the fuel inside the rail to reach the same temperature as the rail wall. The injector parameters such as pulse-width and injection pressure can be controlled and is set to 5 ms and 0.3 MPa, respectively.

ISSN 2176-5480

Atomization parameters are measured by means of Shadowgraphy from LaVision. The illumination is provided by a dual-cavity Nd:YAG laser, 50 mJ pulse and 8 ns duration, 5 Hz frequency, 532 nm wavelength, in conjunction with a dye plate *High Efficiency Diffuser* to backlit the spray. The images are captured by an *Imager Intense* CCD camera, with 1376 x 1040 array, 12 bit digital image and maximum exposure time of 500 ns. A *12X (Ultra) Zoom Lens*, 341 mm of maximum working distance, is attached to the camera to provide high magnifications. A magnification of 1.5 is used in order to reach about 4x3 mm² field of view. A group of 3000 images for each temperature test is chosen to be processed by DAVIS software from Lavision.

The apparatus is shown schematically in Figs. 1 and 2.

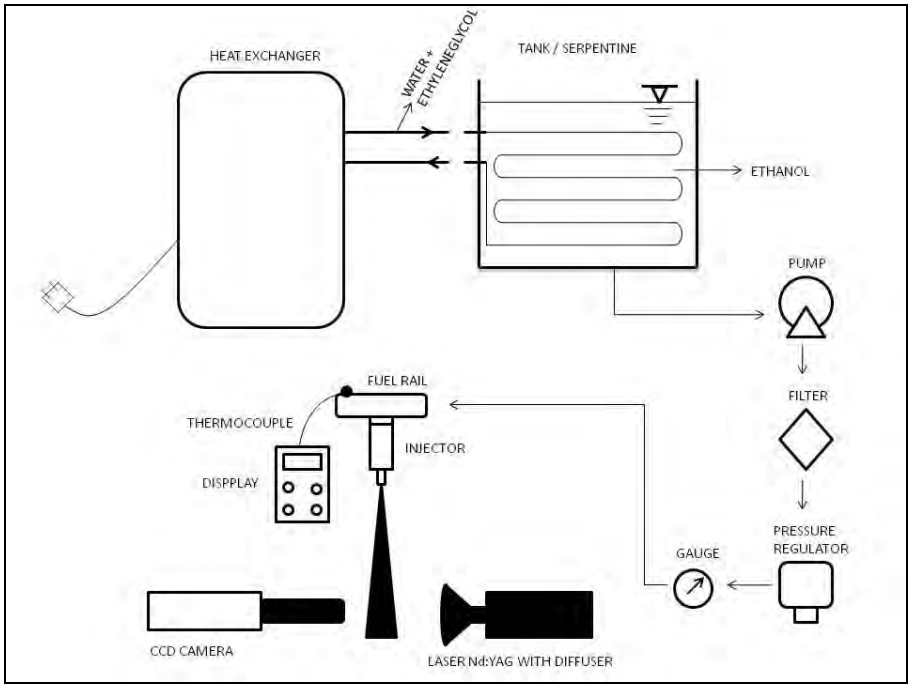

Figure 1. Schematic diagram of experimental apparatus.

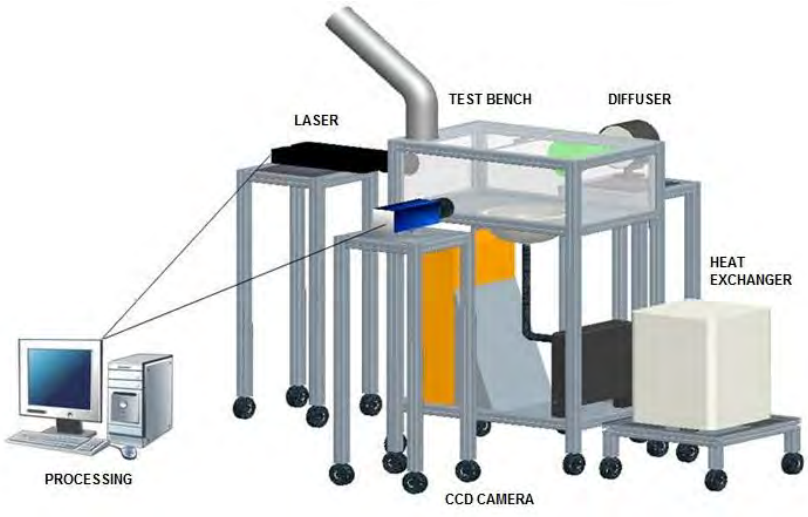

Figure 2. Spray chamber and Shadowgraphy instrumentation.

2.2 Fuel specification

Hydrous ethanol used as vehicle fuel in Brazil was used for the present study. The relevant properties to the spray analysis are on Table 1. All of them were extracted from the fuel supplier specification sheet.

ISSN 2176-5480

Table 1. Ethanol properties.

Fuel Properties	Ethanol
Composition	Ethanol (92.6-93.8 %), water (6.2-7.4%)
Density (kg/m³)[(1)]	0.8093
Surface tension (N/m)[(1)]	0.023
Viscosity (mPa.s)[(1)]	1.64
Boiling point (°C)[(2)]	77

[(1)] measured at 20°C
[(2)] measured at 101 kPa

As viscosity is the fuel property that most vary with temperature, if compared with density and surface tension, the ethanol viscosity was tested as a function of temperature and the result can be seen in Fig. 3. From 10 °C to 60 °C, viscosity changed from 1.97 mPa.s to 0.82 mPa.s, which gives a 58% variation (max. value – min. value/max. value).

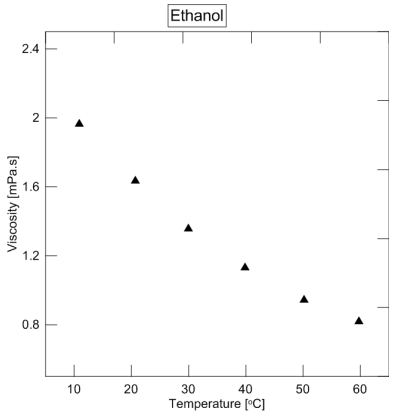

Figure 3. Variation of ethanol viscosity with temperature.

2.3 Fuel injector

A four-hole port fuel injector was designated for the present study. This type of injector contains a pressure-swirl atomizer and produces a conical spray. The injector mass flow is 4.4 g/1000inj (4.4 g per 1000 cycles of injection) at 0.3 MPa fuel pressure, regulated in the fuel rail.

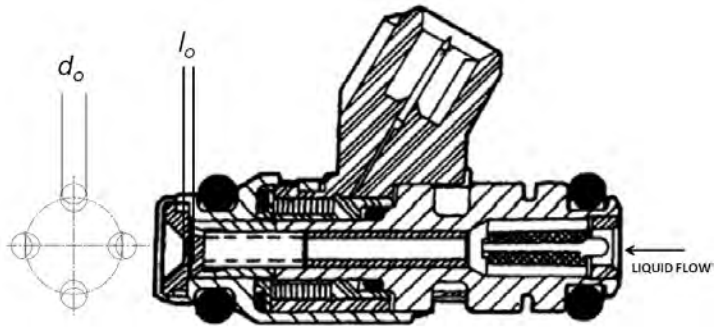

Figure 4. Injector geometry.

The discharge orifice diameter (d_o) is 0.255 mm and the discharge orifice length (l_o) is 0.2 mm. The drop size and velocity field measurements were taken in two different axial positions from the discharge orifice, 25 mm and 100 mm, as can be seen schematically in Fig. 5.

ISSN 2176-5480

Figure 5. Axial distances from nozzle tip.

3. RESULTS AND DISCUSSION

3.1 Processing settings

A preliminary approach concerns to tests performed to set processing and operational parameters in order to find out the best configuration to Shadowgraphy technique.

The Shadowgraphy technique is based on image inversion and detection of intensity levels (gray level), that is the contrast between particles and backlight. A global threshold is used to define the level of contrast that will be used to further segmentation of the accepted image areas. A 50% of global threshold means that regions of the image which have intensity lower than 50% of the maximum intensity are discarded. A low number of threshold allows more particles to be detected, however particles with poorer contrast will be validated. Therefore, a compromise between these two factors must be observed. According to Kim and Kim (1994), selecting a 50% threshold gray level enables particles sizes to be measured accurately due to the existence of a strong linear relationship between the real particle diameter and the measured diameter.

Despite the fact that the Shadow imaging method detects particles by level of contrast it does not necessarily recognize the drop coalescence in all events, so sometimes a group of droplets is depicted as one single particle representing a large diameter. In this case a filter named “ignore diameters above” should be used. The upper limit of diameter is determined by image inspection. Likewise, as the camera resolution is 1376 x 1040 pixels² and the field of view achieved was 4 mm x 3 mm, the pixel size corresponds to 2.9 μm and then a lower limit should be established as well. According to this size of pixel and the precaution that the smallest diameter contains at least 7 pixels inserted, droplets diameters under 20 μm were ignored.

Figure 6 shows part of a processed image where coalescence episodes were not detected by DAVIS software. They are highlighted by a square.

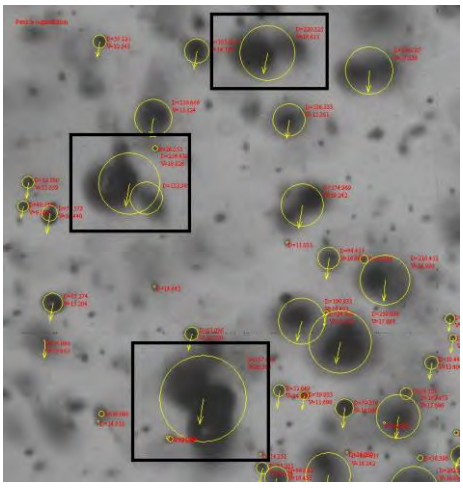

Figure 6. Processed image where coalescence was not denoted.

ISSN 2176-5480

Image analysis shows that values above 250 μm are no longer representative since they usually represent drops where coalescence has occurred.

The injector was tested with static flow (constant voltage delivered to the injector) and dynamic flow (pulsed voltage delivered to the injector, so it opens and closes according to pulse-width) and the results for SMD were compared for both. Repeatability issue was the matter of the tests.

In both cases, static flow and dynamic flow, the results showed quite consistent, therefore it can be said that repeatability was found. The measurements were taken strictly at the same conditions: 100 mm downstream of injector tip, with 0.3 MPa pressure and 20°C temperature. For static flow, collecting a number of 10 measurement points, the maximum variation (maximum value – minimum value/ minimum value) for SMD was approximately 20% and the standard deviation was 4.3 μm. For dynamic flow the maximum variation was 20% as well and the standard deviation was 4.7 μm. It is believed that instabilities such as turbulence, cavitation and even the randomness inherent in the atomization process are the main causes of this small variation, as comment Goldswothy *et al.*, 2011, especially at the axial distance of 25 mm which is very near from the nozzle exit. There are also the experimental errors involved.

The number of images to be taken in each procedure was also evaluated. A number of 3000 images correspond approximately to 30,000 particles detected. It was checked that this is a good sample to obtain accuracy as the SMD fluctuation proved negligible.

3.2 Overall spray form

Figure 7 shows an ethanol spray image at three different times of injection. By image analysis is possible to point out some interesting features. Figure 7(A) presents the initial moment of the liquid getting out of the nozzle, where is possible to notice the presence of ligaments and some vortices.

It is observed that the penetration is a function of injection time, increasing as time increases. Also, it is possible to see the presence of ligaments and larger drops in positions closer to the nozzle tip and smaller drops in distances away from the discharge orifice. This is due to the existence of first and second atomization processes. The first stage of atomization is mainly influenced by instabilities and disruptive forces inherent to the liquid, thus the process is governed by Reynolds number ($\rho_L v_r D/\mu_L$; where ρ_L is liquid density, v_r is the relative velocity between liquid and air, D is drop diameter and μ_L is liquid viscosity), and Weber number ($\rho_L v_L^2 D/\sigma$; where v_L is liquid velocity and σ is surface tension), which provides the capillary instabilities on liquid surface. The second stage of atomization is no longer dependent of Reynolds number as the liquid property that predominates is surface tension. Its role is related with the interaction between aerodynamic forces and surface tension forces. Wang and Lefebvre (1987).

Four jets generated by four-hole fuel injector are clearly seen in initial region of the spray. It is possible to say that the spray morphology and flow characteristics of that section are related to the interaction between the jets, which, in developed region of the spray is not as visible as well, as Anand *et al*., 2012 pointed out.

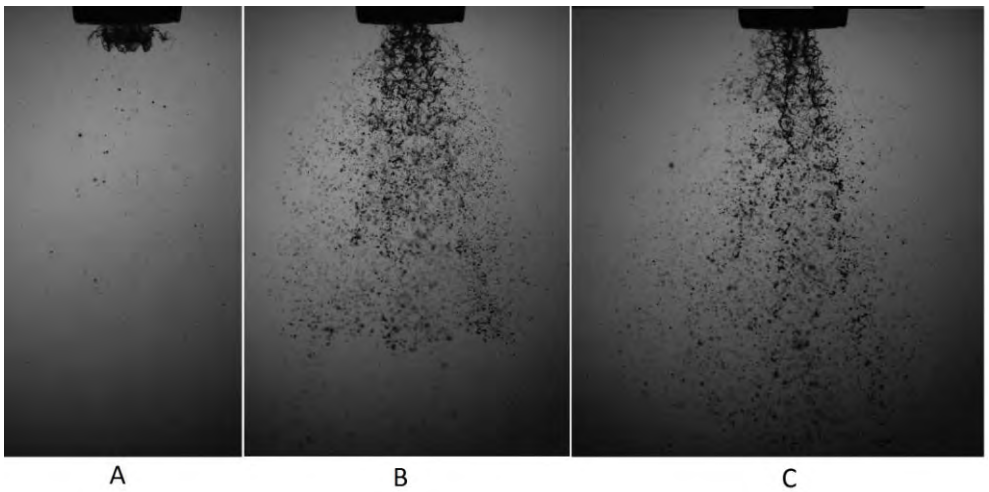

Figure 7. Overall spray form of ethanol in three different times of injection: injection time C > injection time B > injection time A.

ISSN 2176-5480

3.3 Variation of SMD with fuel temperature

Table 2 and 3 show results for SMD for five different fuel temperatures and two different axial positions. The range 10 ^{o}C to 60 ^{o}C was the maximum one achieved since ethanol starts to evaporate, making it impossible to measure with the bench structure used here. It is also possible to see by the number of particles detected in each temperature that from 40 ^{o}C the number decreases abruptly. The explanation for such event is that as fuel begins to evaporate inside the injection chamber the walls start getting blurry and the camera can no longer capture the image faithfully. However, the evaporation does not begin as soon as the liquid is injected; it starts after a while (after approximately 1000 images taken). Therefore, a number of 3000 images is impossible to be selected for that temperatures so than a number of 1000 was picked to 40 ^{o}C and 50 ^{o}C and 700 for 60 ^{o}C. This choice should not affect the accuracy of results since a number of 2000 particles is recommend in order to have convergent statistics.

Table 2. Experimental results for 0.3 MPa injection pressure, 0.1 MPa ambient pressure, 25 mm downstream injector tip position and 5 ms PWM.

Measurements at 25 mm downstream of injector tip			
Heat Exchanger Temperature (^{o}C)	Fuel Temperature (^{o}C)	SMD (μm)	Number of particles detected
10	16	100.5	58178
20	20	139.1	20183
30	28	139.0	23892
40	37	119.2	3706
50	44	121.9	5184
60	55	121.6	5772

Table 3. Experimental results for 0.3 MPa injection pressure, 0.1 MPa ambient pressure, 100 mm downstream injector tip position and 5 ms PWM.

Measurements at 100 mm downstream of injector tip			
Heat Exchanger Temperature (^{o}C)	Fuel Temperature (^{o}C)	SMD (μm)	Number of particles detected
10	16	75.9	19453
20	20	78.6	25709
30	28	75.1	29284
40	37	72.0	26363
50	44	66.8	11232
60	55	70.2	3957

A comparison between measurements made at 25 mm and 100 mm reveals that drops are smaller in distances far away from the injector tip. This is attributed to the fact that second breakup process has occurred so the droplets are expected to be smaller. The SMD values found for each distance also seem consistent with literature for port fuel injection.

Particles were sized for an axial distance of 120 mm only to make sure that 100 mm could be a representative position of spray fully developed region. Images were captured at 20 ^{o}C as all the other operational parameters remained the same. SMD resulted in 70.6 μm which makes a good agreement with those measured at 100 mm, noting that the spray is fully developed there.

Figure 8 shows SMD as function of temperature for each axial distance:

ISSN 2176-5480

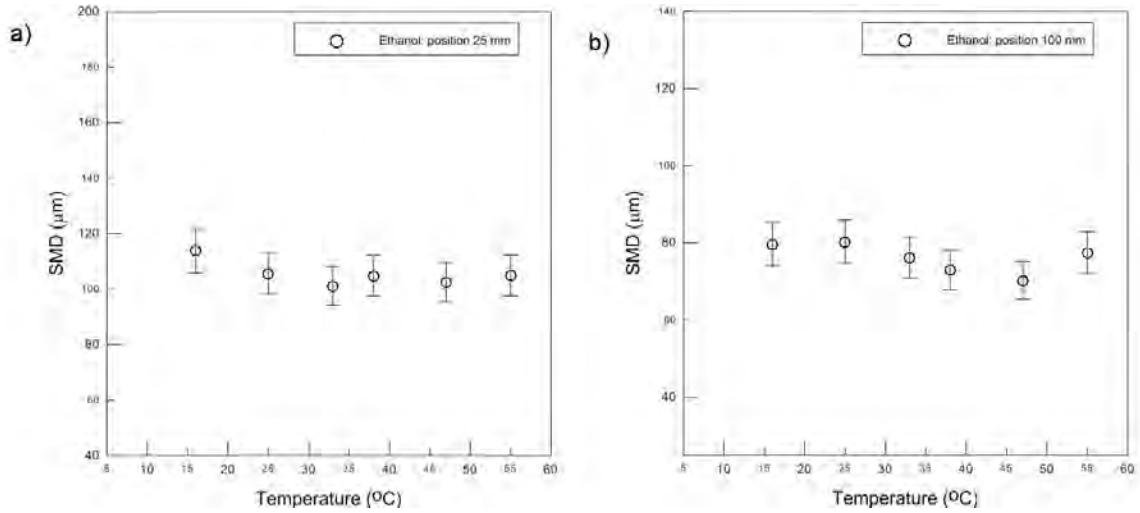

Figure 8. SMD at a) 25 mm and b) 100 mm downstream of injector tip at five distinct temperatures.

With respect to influence of fuel temperature on SMD, for both positions evaluated separately, it is not possible to establish any clear relation between them. The SMD values are close to each other and there is no apparent tendency of their decreasing with increasing temperature possible to validate. Thus is not possible to affirm that temperature influences this atomization parameter.

It is observed that this range (10-60 ^{o}C) provides low variation in fuel properties - viscosity test as function of temperature was demonstrated earlier and ethanol surface tension range from 22.94 mN/m to 20.43 mN/m for the temperature gap of 20-50 ^{o}C, according to Vázquez *et al.*, 1995. Thereat, SMD became insensitive to temperature variation.

3.4 Variation of velocity field with fuel temperature

Figure 9 shows velocities for the two temperature extremes (16 ^{o}C e 55 ^{o}C) as function of diameters. Approximately 4000 points were used to plot.

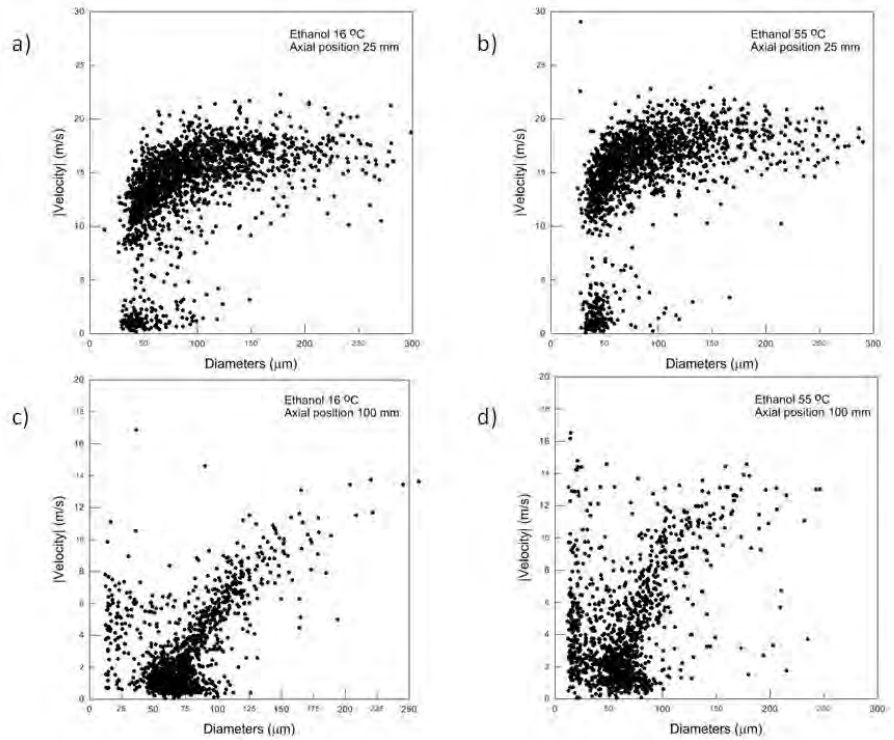

Figure 9. Ethanol drop velocities as function of diameters for (a) 16 ^{o}C, 25 mm (b) 55 ^{o}C, 25 mm (c) 16 ^{o}C, 100 mm (d) 55 ^{o}C, 100 mm.

ISSN 2176-5480

A brief note on the graphs shows that velocities patterns are quite distinct when compared at different axial positions, yet they are quite similar when compared at the same position but at different temperatures.

The velocities at 25 mm downstream of injector tip are primarily concentrated in the range of 10 to 20 m/s, while for the 100 mm position they are condensed from 0 to 10 m/s. Figure 9(a) is alike Fig. 9(b) and Fig. 9(c) is alike Fig. 9(d). It demonstrates that temperature did not influenced particle velocities field.

Important to emphasize that the decrease of velocity as drops move away from discharge orifice occurs due to the action of aerodynamic drag forces. The larger droplets have higher velocities due to the lower drag coefficient. The variation of temperature was not capable of changing the speed because it provided low variation in fuel properties, since drop velocity is affected by the same parameters as its diameter.

4. CONCLUSIONS

Atomization parameters of a port fuel injector in different fuel temperatures have been reported. Ethanol was used as fuel test and measurements were taken into two distinct axial distances from the nozzle tip. Drop sizes and velocities were measured at 0.3 MPa pressure and 5 ms pulse-width using a Shadowgraphy system. The aspects of the spray were also inspected.

Some operational and processing parameters was tested in order to predict the best configuration to measure with the equipment used and it was found that a 50% threshold, a number of 3000 images, a field of view of 4 mm x 3 mm, an upper diameter limit of 250 μm and a lower limit of 20 μm represent a good setting.

SMD seemed to be insensitive to the range of temperature tested because it provided low variation in liquid properties. Likewise, velocities did not seem to sense the temperature variation whereas their profile remained the same for the two extremes plotted.

Regarding the axial position, it is possible to say that 25 mm is representative of first atomization and 100 mm represents second atomization.

5. ACKNOWLEDGEMENTS

I would like to thank Magneti Marelli Powertrain Brazil for the sponsorship, CAPES for the master"s program scholarship, FAEPEX for the research financial support and Laboratory of Chemical Engineering (PQGe) from Unicamp for the space and equipment assigned.

6. REFERENCES

Aleiferis, P. G. et al. *Mechanisms of Spray Formation and Combustion from a Multi-Hole Injector with E85 and Gasoline*. Combustion and Flame, Vol. 157, 2010, pp. 735-756.

Anand, T. N. C., Mohan, A. M., Ravikrishna, R. V. *Spray Characterization of Gasoline-Ethanol Blens from a Multi-Hole Port Fuel Injector*. Fuel, Vol. 102, 2012, pp. 613-623.

Chen, S. K., Lefebvre, A. H., Rollbuhler, J. *Influence of Liquid Viscosity on Pressure-Swirl Atomizer Performance*. Atomization and Sprays, Vol. 1, 1991, pp. 1-22.

Gao, J., Jiang, D., Huang Z. *Spray Properties of Alternative Fuels: A Comparative Analysis of Ethanol-Gasoline Blends and Gasoline*. Fuel, Vol. 86, 2007, pp. 1645-1650.

Goldsworthy, L.C. et al. *Measurements of Diesel Spray Dynamics and the Influence of Fuel Viscosity using PIV and Shadowgraphy*. Atomization and Sprays, Vol. 21, No. 2, 2011, pp. 167-178.

Kim, K. S., Kim, S. S. *Drop Sizing and Depth-of-Field Correction in TV Imaging*. Atomization and Sprays, Vol. 4, 1994, pp. 65-78.

Lee, C. et al. *Spray Structure and Characteristics of High-Pressure Gasoline Injectors for Direct-Injection Engine Applications*. Atomization and Sprays, Vol. 11, No. 2, 2001, pp. 35-48.

Park, S. H. et al. *Atomization and Spray Characteristics of Bioethanol and Bioethanol Blended Gasoline Fuel Injected Through a Direct Injection Gasoline Injector*. International Journal of Heat and Fluid Flow, Vol. 30, 2009, pp. 1183-1192.

Vázquez, G., Alvarez, E., Navaza, J. M. *Surface Tension of Alcohol + Water from 20 to 50 ^{o}C.* J. Chem. Eng. Data, vol. 40, 1995, pp. 611-614.

Wang, X. et al. *Spray Characteristics of High-Pressure Swirl Injector Fueled with Methanol and Ethanol*. Energy and Fuels, Vol. 19, 2005, pp. 2394-2401.

Wang, X. F., Lefebvre, A. H. *Mean Drop Sizes from Pressure-Swirl Nozzles*. Propulsion and Power, Vol. 3, No. 1, 1987, pp. 11-18.

7. RESPONSIBILITY NOTICE

The authors are the only responsible for the printed material included in this paper.